Article:
Taylor, A.F., Tinsley, M.R. and Showalter, K. (2015) Insights into collective cell behaviour from populations of coupled chemical oscillators. Physical Chemistry Chemical Physics , 17 (31). pp. 20047-20055. ISSN: 1463-9076

https://doi.org/10.1039/c5cp01964h

PCCP

Accepted Manuscript

ROYAL SOCIETY OF CHEMISTRY

www.rsc.org/pccp

PCCP

RSCPublishing

Perspective

Insights into collective cell behaviour from populations of coupled chemical oscillators

Cite this: DOI: 10.1039/xoxxooooox

Annette F. Taylor,[a] Mark R. Tinsley[b] and Kenneth Showalter[b]

Received ooth January 2012,
Accepted ooth January 2012

DOI: 10.1039/xoxxooooox

www.rsc.org/

Biological systems such as yeast show coordinated activity driven by chemical communication between cells. Here, we show how experiments with coupled chemical oscillators can provide insights into collective behaviour in cellular systems. Two methods of coupling the oscillators are described: exchange of chemical species with the surrounding solution and computer-controlled illumination of a light-sensitive catalyst. The collective behaviour observed includes synchronisation, dynamical quorum sensing (a density dependent transition to population-wide oscillations), and chimera states, where oscillators spontaneously split into coherent and incoherent groups. At the core of the different types of behaviour lies an intracellular autocatalytic signal and an intercellular communication mechanism that influences the autocatalytic growth.

Introduction

Collective behaviour in biology is a type of self-organisation mediated by communication between individuals within a population. One of the simplest examples of collective behaviour is that of synchronisation of oscillations in organisms that display rhythmical production of chemicals. Synchronisation has fascinated scientists from all disciplines and a number of popular books have been published in the area.[1-3] The emergence of a collective rhythm has been observed at the level of a whole organism, for example in the periodic flashing of fireflies[4], and at the cellular level, such as in the glycolytic oscillations of yeast cells.[5]

Insights into the types of behaviour that might be observed in cellular biological systems displaying chemical oscillations have been obtained using the Belousov-Zhabotinsky (BZ) reaction. The BZ reaction is the most studied chemical oscillator and arguably one of the most studied chemical reactions.[6] Belousov and Zhabotinsky developed an inorganic analogue of the Krebs cycle involving the aqueous phase oxidation of an organic species by acidified bromate in the presence of a metal ion catalyst.[7, 8] The reaction can be monitored by optical imaging or electrochemically as oscillations are accompanied by a change in the colour and oxidation state of the catalyst. A wealth of behaviour, from chemical waves and patterns to chaos, has been observed in experiments. Unlike many biological oscillators, the reaction is sufficiently simple that simulations with models having only two or three variables can reproduce most of the experimental features.

In 1975, motivated by theoretical work on synchronisation of biological oscillators, Stuchl and Marek connected two continuous flow stirred tank reactors (CSTRs) via a perforated plate in the first experiments on coupled chemical oscillators.[9] Each reactor was capable of displaying its own oscillatory dynamics, governed by the inflow rate of reactants for the BZ reaction and the temperature, and was connected to its neighbour by mass exchange. Synchronisation and other more complicated behaviours were observed. Other coupling methods were later explored, such as electrical perturbations of the redox oscillations.[10]

In order to obtain results with more than a few BZ oscillators, miniaturisation of the reaction vessel was required. This was achieved by two means: the compartmentalisation of the reaction in water droplets suspended in oil using a microfluidic reactor[11] and the immobilisation of the catalyst on ion exchange beads. In this paper, we discuss the use of the latter system in investigations of collective behaviour in populations of chemical oscillators. First the experimental methods are described; we then show how synchronisation, dynamical quorum sensing, cluster formation, oscillator death and chimera states arise as a result of the chemical signalling between the individual BZ oscillators.

Experimental methods

Catalytic beads for the BZ reaction

The immobilisation of the metal ion catalyst for the BZ reaction on cation exchange resin beads sparked new possibilities in the investigation of chemical pattern formation far-from-equilibrium.[12, 13] The sulfonated polymer beads can be purchased with a particular size range, or mesh, from approximately 40 μm to 1.2 mm. A quantity of beads is added to a stirred solution of BZ catalyst, such as the iron phenanthroline complex ferroin, giving a typical loading of 1.0 × 10^{-5} moles of catalyst per gram of beads.

The catalytic beads are placed in a bath of solution of the rest of the BZ reagents: sulphuric acid, malonic acid and bromate, with concentrations usually of the order of 0.1 M. The large volume and slow decay of the reagents in the catalyst-free surrounding solution means that the pool chemical approximation can be applied. If the beads are sufficiently small relative to the corresponding reaction-diffusion length scale, each bead may be considered as a uniform micro-reactor, with intermediate concentrations varying according to the reaction kinetics and the rate of transfer to the surrounding solution (Figure 1a).[14]

In the Field, Körös and Noyes (FKN) mechanism[15] of the BZ reaction, the key intermediates are an inhibitor, Br^-, that is removed in process A:

$$BrO_3^- + 5Br^- + 6H^+ \rightarrow 3Br_2 + 3H_2O \quad (1)$$

and an autocatalyst, $HBrO_2$, that catalyses its own production, accompanied by oxidation of the metal ion (M) in process B:

$$BrO_3^- + HBrO_2 + 2M_{red} + 3H^+ \rightarrow 2HBrO_2 + 2M_{ox} + H_2O \quad (2)$$

The bromine produced in process A brominates the malonic acid, and autocatalysis in Process B is curtailed by disproportionation of $HBrO_2$. The inhibitor Br^- is regenerated along with reduction of the metal ion in process C:

$$2M_{ox} + MA + BrMA \rightarrow f\,Br^- + 2M_{red} + \text{other products} \quad (3)$$

where f is a stoichiometric factor that depends on the initial concentrations of bromate and malonic acid. The reaction may remain in a reduced steady state, where process A dominates (low f), change to an oxidised steady state, where process B dominates (high f), or cycle between these two states via process C (intermediate f).

The beads can oscillate for hours, with each bead displaying hundreds of oscillations in the intermediate concentrations, before eventually one of the substrates (malonic acid or bromate) is depleted. The natural frequency or period of oscillations is of the order of minutes and depends on the temperature, the initial concentrations and the individual catalyst loading on a bead. The period also depends on the size of the particles, as the rate of loss of intermediate species from the surface of a bead to the surrounding solution is greater for smaller beads.[16] There is a slow change in the period of the oscillations in time that is negligible during the time-frame of an experiment. The experiments described here were all performed at constant temperature.

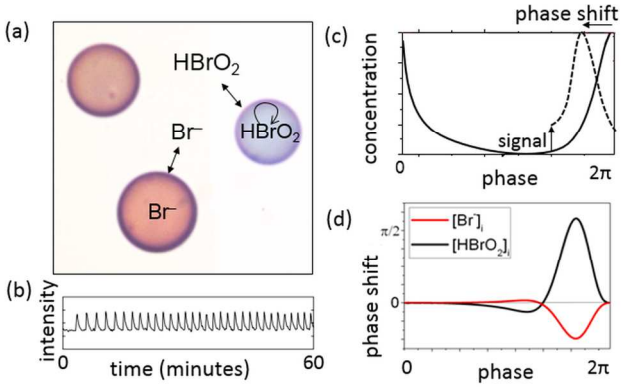

Figure 1. (a) Experimental image of ferroin-loaded catalytic beads in catalyst free BZ solution. The field of view is approximately 1 mm × 1 mm. The reduced catalyst is red (low intensity) and the oxidised catalyst is blue (high intensity). (b) Light intensity-time plot obtained from a series of images of a bead. (c) Sketch of peak to peak oscillation in concentration and corresponding phase of the cycle. Dotted line shows the oscillation after a phase shift in response to a signal. (d) Phase response curve constructed from simulations of the ZBKE model of the BZ reaction[17] showing the phase shift after perturbations in $HBrO_2$ or Br^- at different phases of the cycle.

The amplitude, period and phase of the oscillations are determined from intensity-time plots obtained from images of the beads (Figure 1b). High transmitted light intensity is correlated with the oxidised state of the metal catalyst. There is a rapid increase in intensity associated with autocatalysis in process B and then a slow decrease during process C. The temporal profile of Br^- is similar to that of the metal ion catalyst, whereas there is typically a sharp spike in $HBrO_2$ when process B occurs.

The choice of an appropriate method for the determination of period and phase depends on the complexity of the time series.[2] The instantaneous phase can be obtained by mapping the oscillation onto the complex plane using the analytic signal of the normalised data. The phase may also be defined by linearly scaling the time between successive peaks from 0 to 2π (Figure 1c).

The coupling of BZ oscillators

Two systems are said to be coupled if they interact with each other. This can be distinguished from forcing, in which an external rhythm is imposed on a system.[18]

In the case of BZ oscillators, interaction may result in a change in the amplitude, period and/or phase of the oscillations, driven by a change in the rate of production of the key intermediate species. It is useful to characterise the interaction through the resulting phase shift: a phase advance is defined as a positive phase shift in which an oscillator jumps to a later phase in the cycle, and a phase delay is a negative phase shift in which an oscillator jumps back to an earlier phase. A phase advance is illustrated in Figure 1c. The period of the cycle is reduced compared to the period of the unaffected oscillation.

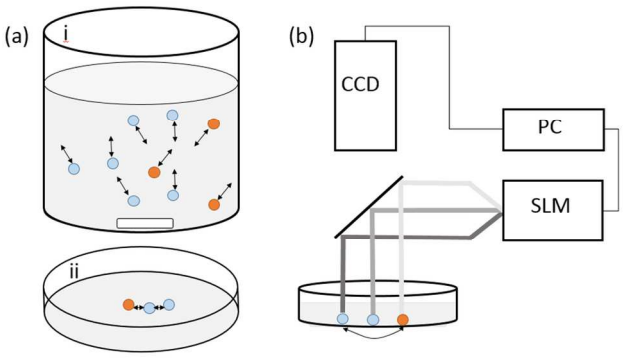

Figure 2. Methods of coupling catalytic BZ beads. (a) Production and emission of chemicals from a bead into the surrounding i) stirred solution (global coupling) and ii) unstirred solution (local coupling). (b) A computer-controlled projected pattern of illumination from a spatial light modulator (SLM) used to obtain non-local coupling.

Phase response curves are frequently used in biology, particularly with neurons, to show the dependency of the phase shift on the phase of the cycle at which a small perturbation was applied. The phase response curve in Figure 1d is constructed from simulations with the Zhabotinsky-Buchholtz-Kiyatkin-Epstein (ZBKE) model of the BZ reaction.[19] This curve shows the phase shift following a small increase in either Br^- or $HBrO_2$ during a single oscillation. Early on in the cycle, the phase shift is virtually zero and the reaction is said to be refractory. When the phase of the cycle is greater than π, an increase of the autocatalyst mainly leads to a phase advance, whereas an increase of the inhibitor leads to a phase delay.

Coupling methods

The BZ catalytic beads may interact with each other through a number of mechanisms. If the reaction medium is stirred, then $HBrO_2$ and Br^- are rapidly stripped from the surface of each bead and transferred to the surrounding solution (Figure 2ai). The concentrations in the surrounding solution can be considered as spatially uniform dynamical variables that depend on the contributions of all the individual beads. This is global or all-to-all coupling. The strength of the coupling depends on a number of factors that affect the rate of transfer, including the stirring rate.

If the solution is not stirred, then during the reaction there is diffusion of $HBrO_2$ and Br^- from a bead to the surrounding solution and other beads (Figure 2aii). Since the concentrations of $HBrO_2$ and Br^- decay in the surrounding solution (through disproportionation and process A), the strength of the coupling is determined by the distance between the beads and the size of the beads relative to the reaction timescale.[20, 21] This is considered nearest neighbour or local coupling in situations where only adjacent beads influence each other.

More complex coupling scenarios can be achieved by use of a light sensitive catalyst such as ruthenium bipyridyl, $Ru(bpy)_3^{2+}$, which absorbs light of wavelength 450 nm:[22]

$$Ru(bpy)_3^{2+} + h\nu \rightarrow Ru(bpy)_3^{2+*} \quad (4)$$

The fate of the activated catalyst on the BZ reaction depends on the initial conditions and can result in photoinhibition or photoexcitation.[23-25] In the studies described here, the latter process dominates; reactions producing autocatalyst occur:[26]

$$Ru(bpy)_3^{2+*} + Ru(bpy)_3^{2+} + BrO_3^- + 3H^+ \rightarrow HBrO_2 + 2Ru(bpy)_3^{3+} + H_2O \quad (5)$$

Using a spatial light modulator (SLM), the light intensity projected on a bead can be varied dynamically according to an algorithm (Figure 2b).[27] If the transmitted light intensity of a particular bead increases, then the intensity of light projected onto a different bead can also be increased, initiating production of $HBrO_2$. The coupling strength depends on the magnitude of the intensity of the projected light. Hence, nonlocal coupling can be achieved, where beads are influenced by signals further away than their immediate neighbours.

Collective behaviour

Synchronisation

Synchronisation of oscillators by local coupling plays an important role in cellular biological systems, for example entrainment of the electrochemical rhythm of cardiac cells by pacemaker cells in the sinoatrial node is vital for the uniform contraction of the heart.[28] The presence of heterogeneities or defects, such as unexcitable tissue, can result in the formation of spirals and a loss of the coordinated chemo-mechanical action.

The slime mould *Dictyostelium discoideum* uses propagating reaction-diffusion waves of cAMP in order to trigger chemotactic aggregation of starving cells: cells move towards the sources of the signalling molecule. It was noted in experiments that two modes of pattern selection were possible: target waves, probably from spontaneously oscillatory sources, or spiral waves. The latter was correlated with a higher cell density in the medium.[29] Model results suggested that the behaviour arose from a slow variation in the dynamics of the cells in time, with cells passing from an excitable to a spontaneously oscillatory state and back to an excitable state.[30]

Diffusion of autocatalyst typically has a synchronising effect: in a thin layer in a Petri dish, a BZ solution develops target waves and the highest frequency wave source entrains the medium with a common rhythm. If a target wave is broken by, for example, dragging a pipette through a wave, spirals form and entrain the medium with the highest possible frequency, as the diffusion of $HBrO_2$ from the tip of the spiral excites the neighbouring medium as soon as it has recovered.[31]

The BZ catalytic beads presented an ideal means to investigate synchronisation of locally coupled oscillators (Figure 2aii), with the ability to characterise the population prior and

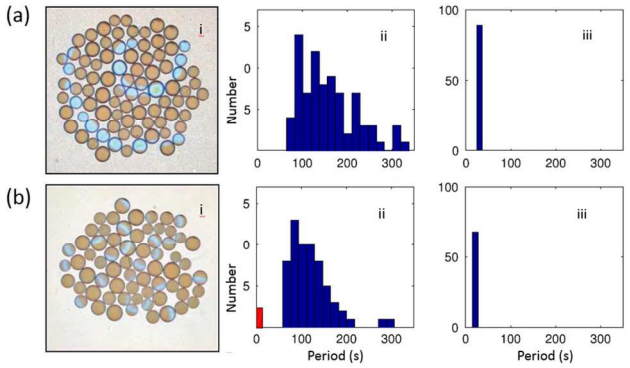

Figure 3. Pattern selection in locally coupled oscillatory beads with (a) low bromate and (b) high bromate concentration. (i) Experimental image, (ii) natural period distribution of the uncoupled beads, i.e., placed more than one bead diameter from each other, and (iii) period of coupled beads. Figure adapted from Ref. [33].

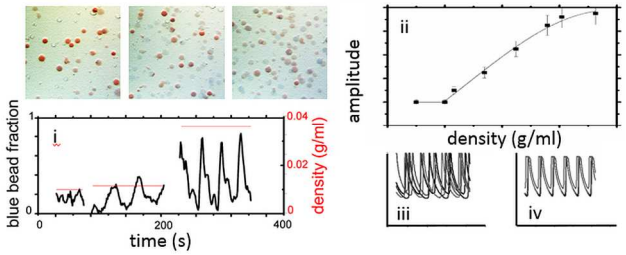

Figure 4. Synchronisation of populations of oscillatory beads with increasing density in stirred solutions at low stirring rates. Images of some of the beads at different densities and (i) fraction of oxidised (blue) beads as a function of time, (ii) the amplitude of the fraction of oxidised beads as a function of density, and simulations of the beads at (iii) low and (iv) high densities showing unsynchronised and synchronised behaviour. Adapted from Ref. 35.

post-coupling.[32] The behaviour was found to depend on the initial concentration of bromate and, hence, the natural periods of the beads (Figure 3a).[33, 34] In a uniform layer of beads, with low concentrations of bromate, pacemakers consisting of a high frequency oscillatory bead or a spiral source entrained all oscillators to have the same period (Figure 3aii). Neighbouring oscillators (away from the core) were phase locked with a fixed phase difference.

As the bromate concentration was increased, an irregular wave pattern appeared that was attributed to the emergence of many spiral sources or re-entrant circuits (Figure 3b), referred to as spiral overcrowding in earlier work. The presence of permanent unexcitable defects may play a role,[36] but there is an alternative explanation. Increasing bromate induced a shift in the natural period distribution of the uncoupled oscillators to lower periods. A detailed analysis revealed that the low period oscillators were refractory for a greater fraction of their oscillatory cycle.[34] Propagating waves of $HBrO_2$ from beads that oxidised rapidly at the start of the reaction were blocked by neighbouring refractory beads. Thus a change in the dynamics of the population of oscillatory beads upon a change in substrate concentration led to the initial phase sensitivity and formation of many spirals.

Numerous studies have indicated that cell density could affect cellular dynamics.[37] This suggested that intercellular coupling may alter the behaviour of individuals within the population. Motivated by these studies, we examined density dependent transitions in stirred suspensions of BZ catalytic beads (Figure 2ai).[35, 38] A particular mass of beads was added to 10.0 ml of solution, giving a number density of beads on the order of 10^5. The oxidation state of the beads was monitored in images of the stirred solution and changes in the intermediate concentrations in the surrounding solution were determined electrochemically using a platinum electrode.

The amplitude of the signal in the surrounding solution was found to increase as the density was increased, but two very different types of transitions were observed (Figure 4 and Figure 5). At low stirring rates, noise was observed in the electrochemical signal at low bead densities (Figure 4). There was a slow growth in the amplitude of the electrochemical oscillations with increasing density. The fraction of blue, oxidised beads was determined from the images as a function of time. Regular oscillations were obtained above a certain density (Figure 4i) and the amplitude of the fraction of oxidised beads gradually increased from one fifth of the population to virtually all of the population (Figure 4ii).

These experimental results combined with model simulations of the reaction (Figure 4iii and iv) revealed that the growth in amplitude at low stirring rates involved gradual synchronization of the chemical oscillators rather than a change in the individual dynamics. In the simulations, the rate of change of autocatalyst on a bead was determined by the reaction kinetics and exchange with the surrounding solution:

$$\frac{\mathrm{d}X_i}{\mathrm{d}t} = -k_{ex}(X_i - X_s) + f(X_i, Y_i, Z_i) \qquad (6)$$

where X_i is the concentration of $HBrO_2$ on a bead, Y_i is the concentration of Br^- and Z_i is the oxidised form of the catalyst. The exchange rate constant k_{ex} is related to the ratio of the surface area to volume of a bead: $k_{ex} = k_{sl}A/V$, where k_{sl} is the solid-liquid mass transfer coefficient. The concentration of $HBrO_2$ in the surrounding solution, X_s, is given by the sum of the contributions from N oscillators:

$$\frac{\mathrm{d}X_s}{\mathrm{d}t} = \frac{\overline{V}}{V_s}\sum_{i}^{N} k_{ex}(X_i - X_s) + g(X_s, Y_s) \qquad (7)$$

where $g(X_s, Y_s)$ contains reaction terms in the catalyst-free solution and $\overline{V}/V_s$ is the dilution factor: the ratio of the average bead volume to the volume of the solution. Typically, an increase in X_s leads to an increase in the rate of production of X on a bead. When a number of oscillators are oxidised together, a pulse of autocatalyst is released into the surrounding solution, which phase advances some of the other responsive oscillators.

As the density is increased, the magnitude of the X_s signal increases, and more of the oscillators join the collective rhythm.

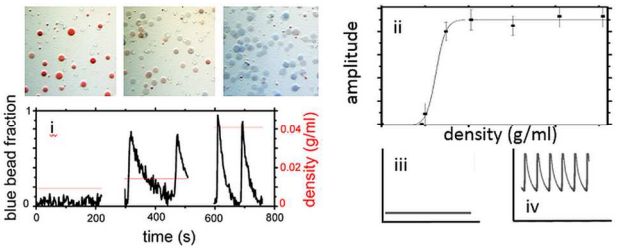

Figure 5. Dynamical quorum sensing with increasing density of BZ beads in stirred solutions at high stirring rates. Images of beads at different densities and (i) fraction of oxidised (blue) beads as a function of time, (ii) the amplitude of the fraction of oxidised beads as a function of density, and simulations of the beads at (iii) low and (iv) high densities, showing no oscillations and synchronised behaviour. Adapted from Ref. [35].

The behaviour of globally coupled oscillators was considered theoretically as far back as the 1960s. Fascinated by the ability of biological systems to synchronise their rhythms, Winfree developed a phase model of globally coupled oscillators.[39] Kuramoto showed that in such a model there exists a critical coupling strength K_c for the emergence of synchronisation that depends on the heterogeneity of the population, i.e., the distribution of natural frequencies.[40] In experiments involving stirred suspensions of oscillatory beads, increasing the number density is equivalent to increasing the global coupling strength. The synchronisation transition is gradual because the oscillators have a wide range of natural frequencies. This is nevertheless a striking example of self-organisation, as the oscillators are synchronised by an internal force generated by the oscillators themselves. The amplitude of the individual oscillators is not altered, just the timing of the rhythms.

Dynamical Quorum Sensing

Quorum sensing in biology refers to a population-wide activity that occurs in single celled organisms in response to an increase in density or number of cells.[41] Cell density affects gene regulation in bacteria with responses such as chemilumilescense and biofilm formation. These organisms share in common with the BZ reaction an autocatalytic production of a species, an autoinducer that is emitted to the surrounding solution, thereby providing a means of chemical communication between the cells. The increase in autoinducer in the surrounding solution with increasing cell density is believed to coordinate activity across the population.

Starved yeast cells display oscillations in glycolytic intermediates with periods on the order of minutes. When out of phase populations were mixed, the global rhythm gradually reappeared, suggesting the cells synchronised their activity through intercellular communication.[42] This was believed to be mediated by acetalehdye. A transition referred to as dynamical quorum sensing was observed in which synchronised oscillations appeared above a critical cell density.[43] It was proposed that none of the cells were oscillating at low cell densities.

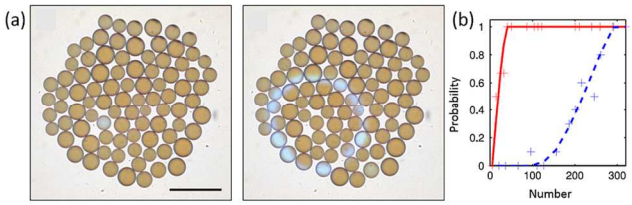

Figure 6. Dynamical quorum sensing in non-oscillatory beads. (a) Images showing appearance of wave activity when beads are locally coupled in a group. (b) Probability of activity as a function of number of beads in the group for bromate 0.3 M (red) and 0.27 M (blue). Figure adapted from Ref. [44].

In the BZ reaction with catalytic beads (Figure 2ai), a transition also was observed with increasing density that involved a change in the dynamics of the individual particles.[35] The electrochemical signal was virtually flat at low bead densities, and above a threshold density, large amplitude oscillations suddenly appeared in the electrochemical signal (Figure 5). The images revealed that there were no oxidised beads at any time at low bead density, and hence no oscillations, but almost all oscillators oxidised together in an oscillatory manner above the critical density.

This transition was observed at higher stirring rates than the gradual synchronisation described earlier. Stirring the solution changes the oscillatory dynamics as it affects the transfer rate of $HBrO_2$ to the surrounding solution: the exchange constant k_{ex} increases with increasing stirring rate. There was a decrease in the rate of production of $HBrO_2$ and when k_{ex} was increased above a critical value, the beads remained in a reduced steady state unable to initiate autocatalysis. If the density of oscillators was increased, there was an increase in the concentration of $HBrO_2$ in the surrounding solution. When the concentration crossed some threshold value, all of the beads suddenly oscillated in complete synchrony.

One of the interesting observations about the transition was the ability of the population to overcome diversity through the coupling. In the model, heterogeneity was obtained through a distribution in a parameter q which regulates local kinetics. The critical density for oscillations in homogeneous populations depended on the value of q. The density at which the heterogeneous population became oscillatory corresponded to that of the average q of the population. Thus all beads became active at the same critical density, irrespective of their underlying differences.

The dynamical quorum sensing transition was also observed in spatially distributed BZ beads.[33, 44] These experiments were designed such that individual beads in solution displayed no oscillations when placed far away from each other. When small numbers of beads were then placed next to each other, no activity was observed. However, the probability of activity increased with increasing numbers of beads and above a

threshold a target or spiral wave source appeared (Figure 6). Simulations suggested that the emergence of activity was associated with a decrease in the loss rate of autocatalyst over the whole population, rather than an increase in the concentration of autocatalyst in the surrounding solution.

Clusters and Multistability

It is somewhat intuitive that populations of globally coupled oscillators might synchronise. Remarkably, oscillators in a stirred solution may also form synchronised groups separated by a phase difference, even though they are all connected by the same surrounding solution. Observed in simulations and theory, these groups are known as phase clusters.[45-47]

Spatial phase clusters were first obtained in experiments with global feedback imposed through the use of light or via the gas phase in the BZ and CO-Pt systems, respectively.[48, 49] In both systems, the spatially extended medium separated into oscillatory regions with a phase lag between them. The first examples of phase clusters in large populations of individual chemical oscillators were achieved using ruthenium-loaded catalytic BZ beads in stirred solutions.[17] In these experiments, the electrochemical signal in the surrounding solution contained two components (Figure 7ai). Analysis of the images of the particles suggested that the signal was generated by two separate groups of oscillators with a phase difference between them, rather than reflecting the dynamics of the individual beads.

Simulations with the model, using parameters for the ruthenium catalyst, showed that the oscillations produced large pulses of bromide ion, so coupling via the inhibitor tended to dominate rather than the autocatalyst. Perturbations with inhibitor result in phase delay (see the phase response curve for Br^- perturbations in Figure 1d). The global signal of bromide in the surrounding solution and on the individual oscillators is shown in Figure 7aii and 7aiii. When the first group of oscillators was oxidised, it emitted a pulse of bromide into the surrounding solution that led to a phase delay of oscillations on the rest of the beads. The number of clusters observed depended on the exchange rate and number density. When either of these parameters was increased, and so the coupling strength was increased, the number of clusters decreased.

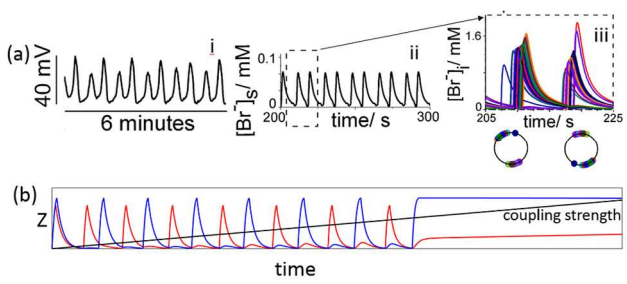

Figure 7. (a) Clusters of synchronised oscillators in stirred solutions of ruthenium-loaded beads. (i) Electrochemical signal in experiments, (ii) bromide concentration in the surrounding solution in simulations and (iii) bromide traces on individual oscillators in simulations, showing two separate groups making up the global signal. Adapted from Ref. 17. (b) Illustration of oscillator death as the coupling strength is increased between two oscillators in simulations with the 3 variable Oregonator model.

A global signal with constant amplitude in time corresponded to a stable configuration, with the oscillators in two groups always firing in the same order. The amplitude of the global signal varied in time in some cases; this corresponded to some of the oscillators jumping between groups by a process of phase repulsion or phase attraction from the global signal. These phase jumpers or "switchers" tend to involve oscillators with high or low natural frequencies.

Theory suggests that populations of globally coupled oscillators may show multi-stability between cluster states such that any number of clusters may coexist for the same parameter.[46, 47, 50] In the experiments involving beads globally coupled via intermediate species emitted to an external solution, there was no evidence of multistability: the initial conditions did not affect the final number of clusters. Coexistence of clusters has been observed in experiments with photosensitive catalytic particles globally coupled by light.[26] In these experiments, groups of up to thirty particles were found to either fully synchronize or form clusters, depending on the initial conditions. The driving force behind the coexistence of states lies in the co-existence of both phase delay and phase attraction in the phase response of the oscillators to $HBrO_2$.[51]

Oscillator Death

The phenomenon of oscillator death is associated with the disappearance of oscillations as a result of the coupling between oscillators.[52, 53] As the coupling strength is increased, the oscillations give way to groups of cells in distinctly different steady states. This transition is of current interest, as it suggests a mechanism for terminal differentiation of a population of cells through intercellular chemical coupling. Oscillations might also be quenched through amplitude death, in which all oscillators collapse to the same steady state as a result of the coupling.[54]

Oscillator death was first observed in experiments with two continuous flow stirred tank reactors (CSTRs) of the BZ reaction coupled by mass transfer.[55] In these experiments, depending on the initial conditions, oscillators synchronised in phase or anti-phase, i.e., they had the same frequency but oscillated

π out of phase with each other. Synchronisation of the anti-phase state was mediated via the inhibitor of the reaction, Br^-. As the coupling strength was increased, the frequency of the anti-phase state decreased and eventually the oscillators attained two opposing steady states, one reduced and one oxidised (illustrated in Figure 7b). In essence, each oscillator was permanently delaying the other. Experiments involving catalyst-loaded beads are not expected to show such a transition because simulations suggest that exchange of the slow variable, the catalyst, is required to stabilise this state.

A related phenomenon to oscillator death is that of Turing patterns, predicted by Alan Turing in perhaps the first

simulations of locally coupled cells in his seminal work on the chemical basis of morphogenesis.[56] The simulations involved autocatalytic and inhibitory species and a key requirement for the observation of the resulting stationary patterns was the fast transport of the inhibitor relative to the autocatalyst. Such patterns have been observed in experiments with BZ droplets suspended in oil in which fast inhibitor diffusion is possible through the oil phase.[57]

Chimera States

The coexistence of states has been demonstrated in populations of nonlocally coupled oscillators. Of particular interest is the Chimera state, in which the population splits into coherent and incoherent groups, so-named after the mythical creature composed of parts from different animals. First predicted theoretically,[58, 59] the Chimera state came as a surprise, as it was obtained with homogeneous oscillators coupled equivalently.

The Chimera state was investigated in experiments with populations of BZ catalytic beads that were nonlocally coupled by light.[60, 61] Figure 8 shows 40 oscillators; each oscillator was coupled to ten others in a 1D ring configuration, with the coupling decreasing in strength with each successive neighbour. (Each oscillator was mapped to a location on a 1D ring and the coupling is then implemented according to its location). The system evolved into two groups, with oscillators 9 to 19 synchronised, and the remainder asynchronous, as shown by the phase of each oscillator at t ~ 1100 s in Figure 8b. Figure 8c shows the variation in the phase of each oscillator as a function of time, with white indicating a value of zero and black a value close to 2π. The oscillators were initiated with a random phase distribution at t = 0. The synchronized group began to form at t ~ 240 s. Once formed the group remained synchronised for the remainder of the experiment, with small fluctuations in the group size.

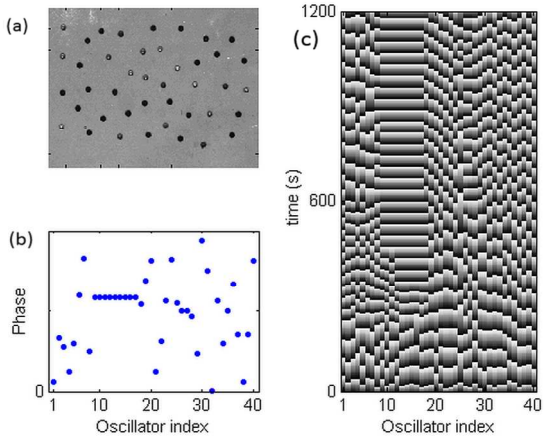

Figure 8. Chimera state in a population of 40 oscillators nonlocally coupled by light. (a) Experimental image: light and dark beads are oscillators in oxidised and reduced state, respectively. (b) Phase of oscillators (indicated by index number) at a particular time. (c) Index vs time plot showing each oscillator's phase represented on a gray scale. Adapted from Ref. [60].

Conclusions and outlook

Much of the early theoretical work on coupled oscillators was inspired by observations of synchronisation in the natural world. This in turn inspired laboratory experiments with relatively simple, well characterised chemical oscillators. These experiments are, to quote Turing (referring to his reaction-diffusion model describing a growing embryo), "an idealization, and consequently a falsification".[56] He nevertheless believed that a discussion of the principles involved would be important in interpreting biological forms. Thus while the complexity of biological environments prevents us from asserting that a behaviour arises from the mechanisms described here, it nevertheless allows us to seek common features that may give rise to similar behaviours. It also allows us to reflect upon what advantages there might be to the mechanisms that biological systems employ, and to whether they might be used in bio-inspired or biomimetic applications.

Collective behaviour can often be explained by consideration of the phase response of oscillators to perturbations.[39, 40] The transition to synchronisation in BZ catalytic bead oscillators connected via an external solution required the release of chemical species. If several oscillators emitted the autocatalyst into the surrounding solution at the same time, that led to a phase advance of some of the other oscillators. Increasing the density increased the magnitude of the global signal, eventually pulling all the oscillators into the collective rhythm.

Remarkably, coupling via a single chemical species in an external solution may also lead to the formation of phase-separated groups of oscillators known as phase clusters. This arose because of the phase-repulsive nature of the coupling when relatively high concentrations of the inhibitor were emitted to the solution. Thus by tuning the wave form of the oscillators, the collective signal might also be controlled.

If the autocatalyst was stripped too quickly from the catalytic beads then oscillations ceased. In this case, an increase of density led to the sudden appearance of synchronised oscillations in a dynamical quorum sensing transition. The transition was a collective one that overcame the diversity of the population. A similar transition was observed in spatially distributed non-oscillatory beads. The probability of wave activity increased as the number of beads increased, driven by the reduction in loss rate of autocatalyst to the surrounding solution.

Autocatalytic signals propagate undamped through systems of locally coupled oscillators over length scales orders of magnitude larger than cells. However, we have shown here that reaction-diffusion does not necessarily result in phase locking of neighbouring cells: complex spatiotemporal patterns arise in oscillators with relatively long refractory periods.

Many single-celled organisms, such as yeast, bacteria and slime mould show population-wide dynamics. These cellular systems share in common with the experiments described here the combination of an autocatalytic signal and an intercellular

communication mechanism. The presence of autocatalysis ensures the possibility for a response above a threshold signal; sharp thresholds exist in systems maintained far from equilibrium containing unstable states.[62, 63] It also provides a mechanism by which behaviour can be rapidly synchronised across a population. The population-wide switches and synchronisation of activity are used by cellular organisms to deliver coordinated pulses of chemicals, initiate motion and material formation. Synchrony plays a vital role in living systems despite external fluctuations, or may even be enhanced by them.[28]

Here, we have demonstrated how the combination of experiments and simulations with simple models of the BZ reaction on catalytic beads can provide insights into collective behaviour. Other types of oscillators have also generated illuminating results, such as the electrochemical systems explored by Kiss et al.[64-66] and Krischer et al.[67, 68] The advantage to the system described here was the ability to work with large numbers of oscillators. The BZ system is the only reaction to display long lived chemical oscillations in a closed reactor, therefore making it the muse of many experiments inspired by nature.[69] However, the harsh chemicals involved in this inorganic analogue of the Krebs cycle preclude its use for applications in living systems.

With advances taking place in synthetic biology, our ability to control the behaviour of cellular biological systems has never been greater and the collective behaviours described here have now been obtained in genetically modified organisms. Simulations suggested that genetic oscillators may synchronize their activity when connected via an extracellular solution;[70] recent experiments showed that *E. coli* may be genetically rewired to exhibit oscillations and synchronize by such a mechanism.[71] A different approach to bio-based collective behaviour involves the design of autocatalysis based on biological molecules such as DNA, peptides and enzymes.[72-76] The compartmentalisation of these synthetic autocatalytic reactions and oscillators may provide new methods for drug delivery, sensing and repair that may be exploited in living systems.

Acknowledgements

This work was supported by National Science Foundation grant CHE-1212558 (KS) and UK Engineering and Physical Sciences Research Council grant GR/T11036/01 (AFT).

Notes and references

[a] Chemical and Biological Engineering, Mappin Street, University of Sheffield.

[b] C. Eugene Bennett Department of Chemistry, West Virginia University, Morgantown, West Virginia 26506-6045, USA.

1. S. Strogatz, *Sync: The emerging science of spontaneous order*, Hyperion, New York, 2003.
2. A. S. Pikovsky, M. Rosenblum and J. Kurths, *Synchronization: A universal concept in nonlinear sciences*, Cambridge University Press, Cambridge, 2001.
3. S. C. Manrubia, A. S. Mikhailov and D. H. Zannette, *Emergence of Dynamical Order: Synchronization Phenomena in Complex Systems*, World Scientific Publishing Company, Singapore, 2004.
4. J. Buck, *Q. Rev. Biol.*, 1988, **63**, 265-289.
5. S. Dano, F. Hynne, S. De Monte, F. d'Ovidio, P. G. Sorensen and H. Westerhoff, *Faraday Discuss.*, 2001, **120**, 261-276.
6. I. R. Epstein and J. A. Pojman, *An introduction to nonlinear chemical dynamics: oscillations, waves, patterns and chaos*, Oxford University Press, New York, 1998.
7. B. P. Belousov, *Sbornik Referatov po Radiatsionni Meditsine*, 1958, 145.
8. A. M. Zhabotinsky, *Biofizika*, 1964, **9**, 306.
9. M. Marek and I. Stuchl, *Biophys. Chem.*, 1975, **3**, 241-248.
10. M. F. Crowley and R. J. Field, *J. Phys. Chem.*, 1986, **90**, 1907-1915.
11. M. Toiya, V. K. Vanag and I. R. Epstein, *Angew. Chem. Int. Ed.*, 2008, **47**, 7753-7755.
12. J. Maselko, J. S. Reckley and K. Showalter, *J. Phys. Chem.*, 1989, **93**, 2774-2780.
13. J. Maselko and K. Showalter, *Nature*, 1989, **339**, 609.
14. R. Aihara and K. Yoshikawa, *J. Phys. Chem. A*, 2001, **105**, 8445-8448.
15. R. J. Field, E. Körös and R. M. Noyes, *J. Am. Chem. Soc.*, 1972, **94**, 8649.
16. K. Yoshikawa, R. Aihara and K. Agladze, *J. Phys. Chem. A*, 1998, **102**, 7649-7652.
17. A. F. Taylor, M. R. Tinsley, F. Wang and K. Showalter, *Angew. Chem. Int. Ed.*, 2011, **50**, 10161-10164.
18. V. Petrov, Q. Ouyang and H. L. Swinney, *Nature*, 1997, **388**, 655-657.
19. A. M. Zhabotinsky, F. Buchholtz, A. B. Kiyatkin and I. R. Epstein, *J. Phys. Chem.*, 1993, **97**, 7578-7584.
20. N. Nishiyama and K. Eto, *J. Chem. Phys.*, 1994, **100**, 6977-6978.
21. K. Miyakawa, T. Okabe, M. Mizoguchi and F. Sakamoto, *J. Chem. Phys.*, 1995, **103**, 9621-9625.
22. R. Toth and A. F. Taylor, *Prog. React. Kinet. Mech.*, 2006, **31**, 59-115.
23. I. Hanazaki, *J. Phys. Chem.*, 1992, **96**, 5652-5657.
24. T. Amemiya, T. Ohmori and T. Yamaguchi, *J. Phys. Chem. A*, 2000, **104**, 336-344.
25. S. Kadar, T. Amemiya and K. Showalter, *J. Phys. Chem. A*, 1997, **101**, 8200-8206.
26. A. F. Taylor, P. Kapetanopoulos, B. J. Whitaker, R. Toth, L. Bull and M. R. Tinsley, *Phys. Rev. Lett.*, 2008, **100**, 4.
27. S. Kadar, J. C. Wang and K. Showalter, *Nature*, 1998, **391**, 770-772.
28. L. Glass, *Nature*, 2001, **410**, 277.
29. K. J. Lee, E. C. Cox and R. E. Goldstein, *Phys. Rev. Lett.*, 1996, **76**, 1174-1177.
30. J. Lauzeral, J. Halloy and A. Goldbeter, *Proc. Natl. Acad. Sci. U.S.A.*, 1997, **94**, 9153-9158.
31. A. T. Winfree, *Science*, 1972, **175**, 634.
32. H. Fukuda, H. Morimura and S. Kai, *Physica D*, 2005, **205**, 80-86.
33. M. R. Tinsley, A. F. Taylor, Z. Huang, F. Wang and K. Showalter, *Physica D*, 2010, **239**, 785-790.
34. M. R. Tinsley, A. F. Taylor, Z. Huang and K. Showalter, *Phys. Chem. Chem. Phys.*, 2011, **13**, 17802-17808.
35. A. F. Taylor, M. R. Tinsley, F. Wang, Z. Huang and K. Showalter, *Science*, 2009, **323**, 614-617.
36. R. Toth and A. F. Taylor, *J. Chem. Phys.*, 2006, **125**.
37. H. G. Othmer and J. A. Aldridge, *J. Math. Biol.*, 1978, **5**, 169-200.
38. R. Toth, A. F. Taylor and M. R. Tinsley, *J. Phys. Chem. B*, 2006, **110**, 10170-10176.
39. A. T. Winfree, *J. Theor. Biol.*, 1967, **16**, 15-&.
40. Y. Kuramoto, *Chemical Oscillations, Waves and Turbulence*, Springer, Berlin, 1984.

41. M. B. Miller and B. L. Bassler, *Annu. Rev. Microbiol.*, 2001, **55**, 165-199.
42. P. Richard, B. M. Bakker, B. Teusink, K. vanDam and H. V. Westerhoff, *Eur. J. Biochem.*, 1996, **235**, 238-241.
43. S. De Monte, F. d'Ovidio, S. Dano and P. G. Sorensen, *Proc. Natl. Acad. Sci. U.S.A.*, 2007, **104**, 18377-18381.
44. M. R. Tinsley, A. F. Taylor, Z. Y. Huang and K. Showalter, *Phys. Rev. Lett.*, 2009, **102**, 4.
45. D. Golomb, D. Hansel, B. Shraiman and H. Sompolinsky, *Phys. Rev. A*, 1992, **45**, 3516-3530.
46. D. Hansel, G. Mato and C. Meunier, *Phys. Rev. E*, 1993, **48**, 3470-3477.
47. K. Okuda, *Physica D*, 1993, **63**, 424-436.
48. V. K. Vanag, L. F. Yang, M. Dolnik, A. M. Zhabotinsky and I. R. Epstein, *Nature*, 2000, **406**, 389-391.
49. M. Kim, M. Bertram, M. Pollmann, A. von Oertzen, A. S. Mikhailov, H. H. Rotermund and G. Ertl, *Science*, 2001, **292**, 1357-1360.
50. H. Daido, *J. Phys. A: Math. Gen.*, 1995, **28**, L151-L157.
51. A. F. Taylor, P. Kapetanopoulos, B. J. Whitaker, R. Toth, L. Bull and R. Tinsley, *Eur. Phys. J. Spec. Top.*, 2008, **165**, 137-149.
52. D. G. Aronson, G. B. Ermentrout and N. Kopell, *Physica D-Nonlinear Phenomena*, 1990, **41**, 403-449.
53. K. Bar-Eli, *Physica D-Nonlinear Phenomena*, 1985, **14**, 242-252.
54. A. Koseska, E. Volkov and J. Kurths, *Phys. Rep.-Rev. Sec. Phys. Lett.*, 2013, **531**, 173-199.
55. M. F. Crowley and I. R. Epstein, *J. Phys. Chem.*, 1989, **93**, 2496.
56. A. M. Turing, *Philos. Trans. R. Soc. Lond. Ser. B-Biol. Sci.*, 1952, **237**, 37-72.
57. N. Tompkins, N. Li, C. Girabawe, M. Heymann, G. B. Ermentrout, I. R. Epstein and S. Fraden, *Proc. Natl. Acad. Sci. U.S.A.*, 2014, **111**, 4397-4402.
58. Y. Kuramoto and D. Battogtokh, *Nonlinear Phenomena in Complex Systems*, 2002, **5**, 380-385.
59. D. M. Abrams and S. H. Strogatz, *Phys. Rev. Lett.*, 2004, **93**, 4.
60. S. Nkomo, M. R. Tinsley and K. Showalter, *Phys. Rev. Lett.*, 2013, **110**, 5.
61. M. R. Tinsley, S. Nkomo and K. Showalter, *Nature Phys.*, 2012, **8**, 662-665.
62. J. J. Tyson, K. C. Chen and B. Novak, *Curr. Opin. Cell Biol.*, 2003, **15**, 221-231.
63. D. Witters, B. Sun, S. Begolo, J. Rodriguez-Manzano, W. Robles and R. F. Ismagilov, *Lab. Chip*, 2014, **14**, 3225-3232.
64. I. Z. Kiss, C. G. Rusin, H. Kori and J. L. Hudson, *Science*, 2007, **316**, 1886-1889.
65. M. Wickramasinghe and I. Z. Kiss, *Phys. Chem. Chem. Phys.*, 2014, **16**, 18360-18369.
66. W. Wang, I. Z. Kiss and J. L. Hudson, *Phys. Rev. Lett.*, 2001, **86**, 4954-4957.
67. K. Schoenleber, C. Zensen, A. Heinrich and K. Krischer, *NJPh*, 2014, **16**.
68. L. Schmidt, K. Schoenleber, K. Krischer and V. Garcia-Morales, *Chaos*, 2014, **24**.
69. I. R. Epstein, V. K. Vanag, A. C. Balazs, O. Kuksenok, P. Dayal and A. Bhattacharya, *Acc. Chem. Res.*, 2012, **45**, 2160-2168.
70. J. Garcia-Ojalvo, M. B. Elowitz and S. H. Strogatz, *Proc. Natl. Acad. Sci. U.S.A.*, 2004, **101**, 10955-10960.
71. T. Danino, O. Mondragon-Palomino, L. Tsimring and J. Hasty, *Nature*, 2010, **463**, 326-330.
72. S. N. Semenov, A. S. Y. Wong, R. M. van der Made, S. G. J. Postma, J. Groen, H. W. H. van Roekel, T. F. A. de Greef and W. T. S. Huck, *Nat. Chem.*, 2015, **7**, 160-165.
73. N. Wagner, S. Alasibi, E. Peacock-Lopez and G. Ashkenasy, *J. Phys. Chem. Lett.*, 2015, **6**, 60-65.
74. S. Otto, *Acc. Chem. Res.*, 2012, **45**, 2200-2210.
75. F. Muzika, T. Bansagi, I. Schreiber, L. Schreiberova and A. F. Taylor, *Chem. Commun.*, 2014, **50**, 11107-11109.
76. A. Padirac, T. Fujii, A. Estevez-Torres and Y. Rondelez, *J. Am. Chem. Soc.*, 2013, **135**, 14586-14592.

Table of Contents Figures